Amphotericin B channels in phospholipid membrane-coated nanoporous silicon surfaces: Implications for photovoltaic driving of ions across membranes

Solomon Yilma[a], Nangou Liu[b], Alexander Samoylov[a], Ting Lo[a],
C. Jeffrey Brinker[c,d], Vitaly Vodyanoy[a,*]

[a] Department of Anatomy, Physiology and Pharmacology, 109 Greene Hall, Auburn University, Auburn, AL 36849, USA
[b] Department of Electrical Engineering, Auburn University, Auburn, AL 36849, USA
[c] University of New Mexico, Center for Micro-Engineered Materials, Albuquerque, NM, USA
[d] Sandia National Laboratory, Albuquerque, NM, USA

Abstract

The antimycotic agent amphotericin B (AmB) functions by forming complexes with sterols to form ion channels that cause membrane leakage. When AmB and cholesterol mixed at 2:1 ratio were incorporated into phospholipid bilayer membranes formed on the tip of patch pipettes, ion channel current fluctuations with characteristic open and closed states were observed. These channels were also functional in phospholipid membranes formed on nanoporous silicon surfaces. Electrophysiological studies of AmB–cholesterol mixtures that were incorporated into phospholipid membranes formed on the surface of nanoporous (6.5 nm pore diameter) silicon plates revealed large conductance ion channels (∼300 pS) with distinct open and closed states. Currents through the AmB–cholesterol channels on nanoporous silicon surfaces can be driven by voltage applied via conventional electrical circuits or by photovoltaic electrical potential entirely generated when the nanoporous silicon surface is illuminated with a narrow laser beam. Electrical recordings made during laser illumination of AmB–cholesterol containing membrane-coated nanoporous silicon surfaces revealed very large conductance ion channels with distinct open and closed states. Our findings indicate that nanoporous silicon surfaces can serve as mediums for ion-channel-based biosensors. The photovoltaic properties of nanoporous silicon surfaces show great promise for making such biosensors addressable via optical technologies.
© 2006 Elsevier B.V. All rights reserved.

Keywords: Amphotericin B; Cholesterol; Nanoporous surfaces; Photovoltaic

1. Introduction

Amphotericin B (AmB) is a polyene macrolide antibiotic that is widely used for its antifungal activity, despite its undesirable side effects (Hartsel and Bolard, 1996). In biological systems, AmB acts by forming ion channels that induce ion leakage across lipid membranes (Bolard, 1986; Holz and Finkelstein, 1970). The formation of these channels is highly dependent on the presence of sterols (cholesterol or ergosterol) in the membrane (Kerridge and Whelan, 1983). The sterol molecules facilitate the assembly of the channel by acting as 'glue' or 'zipper' that links the AmB monomers together in a channel-forming configuration. Displacement of this sterol 'zipper' results in the disassembly of the channel, thereby blocking ion transport across the membrane. The electrophysiological properties of AmB channels in lipid bilayer membranes have been extensively studied in the past in order to elucidate their mechanism of action (Ermishkin et al., 1976, 1977; Borisova et al., 1979; Brutyan and McPhie, 1996). However, little if any research has focused on studying the function of AmB channels in membranes formed on solid substrates. Efforts to construct ion-channel-based stochastic sensors (Bayley et al., 2000; Schuster et al., 1998; Gu et al., 1999) in recent years have shed light on the potential of ion channels for use as transducers in biosensors. The principal emphasis has been on biosensors based on ion channels inserted into supported lipid bilayers (Pantoja et al., 2001; Peterman et

al., 2002; Becucci et al., 2005; Gong and Lin, 2003; Ma et al., 2003; Urisu et al., 2005; Wilk et al., 2004) reviewed by Anrather et al. (2004).

A silicon wafer can be used as a substrate for deposition of membranes that are carrying ion channels or ion carriers. These channels serve as switching elements that convert a binding event into electrical signal and function as transducers in biosensors. When a small voltage is applied to a membrane on the surface of a substrate containing a channel with a specific analyte is bound, an ion channel opens and a small current pulse through the channel indicates the binding event. The molecules used as channels are usually quite small and their density on the wafer surface is high, thus making the addressing of these channels very difficult.

The conventional solution for this problem would be to make electrical connections to all or many of these channels. The applied voltage and responses of individual addresses on the wafer surface can be scanned with the help of computerized circuitry (Vodyanoy, 1998). However, the resolution of these addressable electrodes is poor, and manufacturing of electrode system on the substrate surface may be difficult and expensive.

In this work, we build upon our previous findings (Sykora et al., 2003; Yilma et al., in press) about the ion channel forming properties of the AmB–cholesterol complex to further explore the functioning of these channels on phospholipid membrane-coated nanoporous silicon surfaces. We have previously shown that AmB and cholesterol form highly conductive ion channels in tip–dip phospholipid bilayers. The most stable monolayers were produced from molecules of AmB and cholesterol mixture with 2:1 stoichiometry. At this ratio, AmB and cholesterol interact to form ion channels in lipid bilayers with millisecond dwell times and conductances of 4–400 pS. The AmB–cholesterol complexes assemble in three, four, etc. subunit aggregates to form ion channels of diverse and large conductances. Their I–V characteristics were linear over a range of ±200 mV. The channel currents were inhibited by the addition of tetraethylammonium (TEA) to the cis-side of the membrane. Likewise, AmB–cholesterol complexes reconstituted in membrane-coated nanoporous silicon dioxide surfaces showed single channel behavior with large amplitudes at various voltages. These large-conductance ion channels show great promise for use in biosensors on solid support. Here we present further evidence of these channels functioning in phospholipid membrane-coated nanoporous silicon surfaces (Lu et al., 1997; Brinker et al., 1999) and show photovoltaic potentials generated when the nanoporous silicon surfaces are illuminated with a narrow laser beam can be used to drive ions through the channels. Thus we demonstrate optically addressable ion channels on solid substrate.

2. Materials and methods

2.1. Materials

Amphotericin B was purchased from Sigma Co. (St. Louis, MO) in powder form. Cholesterol and 1,2-diphytanoyl-sn-glycero-3-phosphocholine solutions were purchased from Avanti Polar Lipids (Alabaster, AL). Both were used with-

out further purification. Chloroform (99+% purity), methanol (99+% purity), and hexane (95+% purity) were all purchased from Aldrich Chemical Company (Milwaukee, WI) in bottles packaged under nitrogen. Tetraethylammonium chloride (TEA) was also purchased from Aldrich Chemical Company in crystalline form. Nanoporous (~6.5 nm pore diameter) silica membrane (~300 nm thickness) coated glass/silicon plates were supplied by Dr. C.J. Brinker at the Sandia National Laboratory. The 635 nm diode laser (<1 mW) was purchased from Edmund Industrial Optics (Barrington, NJ).

2.2. Reconstitution of amphotericin B–cholesterol channels in lipid bilayers

Lipid bilayers containing pure 1,2-diphytanoyl-sn-glycero-3-phosphocholine were formed on the tip of patch pipettes using the tip–dip technique previously described (Suppiramaniam et al., 2001; Vodyanoy et al., 1993). The bilayers were formed in asymmetric saline condition by the successive transfer of two lipid monolayers on the tip of the patch pipette. The pseudo-extracellular solution (bathing the cis-side of the membrane) contained 125 mM NaCl, 5 mM KCl, 1.25 mM NaH$_2$PO$_4$, and 5 mM Tris–HCl at pH 7.4, while the pseudo-intracellular solution (inside the patch pipette) contained 110 mM KCl, 4 mM NaCl, 2 mM NaH$_2$CO$_3$, 0.1 mM CaCl$_2$, 1 mM MgCl$_2$, and 2 mM MOPS at pH 7.4. A 2:1 (mol/mol) mixture of 0.6 μg AmB and 0.12 μg cholesterol dissolved in a chloroform–methanol (2:1, v/v) solvent was sonicated together with 10 μg phospholipid (in hexane) and 10 μL of pseudo-extracellular solution in order to form liposomes. (The mass of 2 mol of AmB is ~5 times as large as that of 1 mol of cholesterol.) The emulsion was then carefully transferred to the surface (air–water interface) of the pseudo-extracellular solution bathing the cis-side of the membrane and allowed to equilibrate for 1 min. Incorporation of AmB–cholesterol into the membrane was achieved by dipping the tip of the patch pipette into the emulsion. The membrane incorporated AmB–cholesterol channels were subjected to conventional electrophysiological (Suppiramaniam et al., 2001; Vodyanoy et al., 1993) studies at room temperature (~22 °C). The resulting single channel current fluctuations were filtered at 1 or 5 kHz using a lowpass Bessel filter and recorded on VHS tapes for later analysis. Single channel fluctuations elicited by the AmB–cholesterol complexes were subsequently blocked by the addition of tetraethylammonium (TEA) to the pseudo-extracellular solution on the cis-side of the membrane.

2.3. Reconstitution of amphotericin B–cholesterol channels in membrane-coated nanoporous surfaces

A 150 (l aliquot of AmB, cholesterol, and 1,2-diphytanoyl-sn-glycero-3-phosphocholine mixture (2:1:2, mol/mol ratio, respectively) dissolved in a chloroform/methanol (2:1, v/v) solvent at 0.24 mg/ml concentration was spread on the subphase surface. The monolayer was allowed to equilibrate and stabilize for 10 min at 19 ± 0.1 °C. It was then compressed at a rate of 30 mm/min, and a vertical film deposition was carried out at a rate of 4.5 mm/min and a constant surface pressure
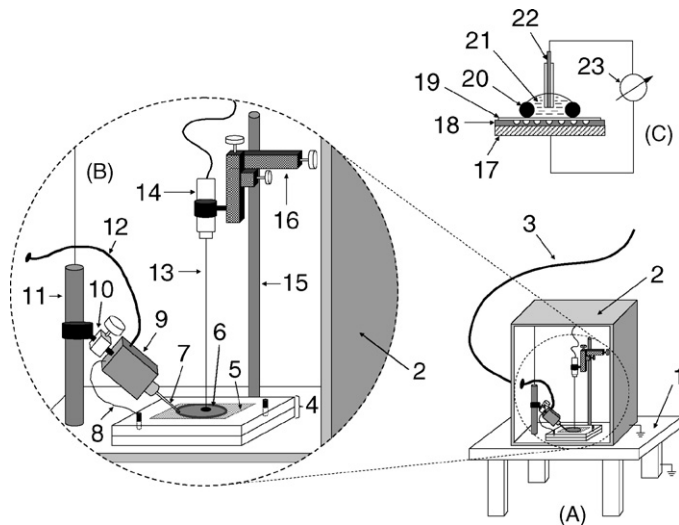
Fig. 1. Setup for studying ion channels in membrane-coated nanoporous silicon surfaces. A modified patch-clamp setup can be utilized to study ion channels that have been incorporated in membrane-coated nanoporous silicon surfaces. Panel A depicts the modified patch-clamp assembly with the components identified as follows: (1) isolation table; (2) Faraday box; (3) input to patch-clamp amplifier. Panel B shows a magnified view of the components inside the Faraday box (2) as follows: (4) plastic cell assembly; (5) nanoporous silicon plates; (6) O-ring; (7) recording electrode; (8) reference electrode and input; (9) head stage; (10) micromanipulator; (11) metal stand; (12) input to patch-clamp amplifier; (13) laser beam; (14) 635 nm diode laser; (15) metal stand; (16) micromanipulator. Panel C depicts a simplified schematic of the nanoporous silicon plates and plastic cell assembly as follows: (17) silicon plate; (18) nanoporous surface; (19) lipid membrane; (20) rubber O-ring; (21) electrolyte solution; (22) Ag/AgCl recording electrode; (23) voltage-clamp connection. The voltage (potential) for driving the ions can be directly applied through the patch-clamp amplifier, or indirectly generated by illuminating the surface of the nanoporous silicon plates with a beam from a diode laser.

of 23 mN/m. Mixed phospholipid monolayers were transferred onto (22 mm × 22 mm) nanoporous (∼6.5 nm) silica membrane-coated glass/silicon plates (Sandia National Lab). The reservoirs in the nanopores were first filled with Langmuir–Blodgett (LB) buffer solution (55 mM KCl, 0.1 mM $CaCl_2$, 1 mM $MgCl_2$, 4 mM NaCl, and 2 mM 3-(N-morpholino) propanesulfonic acid (MOPS), pH 7.4) (Yilma et al., in press) before being coated with phospholipid membranes. The phospholipid membrane-coated nanoporous plate was then secured in place by a plastic cell assembly (Fig. 1B and C) which isolated the center of

the plate with a rubber O-ring. The surface of the nanoporous plate was covered with a small pool of 0.1 M KCl buffer solution, and the entire plastic cell assembly was placed inside a grounded metal box (Fig. 1A) that was positioned on an isolation table GS-34 (Newport Corp.). The plastic cell assembly was connected to an Axopatch 200B patch clamp amplifier (Axon Instruments) by immersing a silver/silver chloride electrode into the small pool (300 μl) of aqueous KCl solution. The voltage clamp amplifier was interfaced to a computer with a Digidata 1200 data acquisition board (Axon Instruments). Current measurements were performed in the dark with the voltage clamped at −200 to +200 mV range. Additional current measurements were performed (without clamping the voltage) while illuminating the nanoporous silicon surfaces with a narrow laser beam (Fig. 1B) from a 635 nM diode laser.

2.4. Data analysis

Single channel data segments of 5–120 s lengths were digitized at 0.1 ms intervals and transferred to a computer as data files. The data were later subjected to statistical analysis using the Fetchan/Clampfit modules of pCLAMP data analysis program (Axon Instruments) as well as the Microcal Origin data analysis and technical graphics program.

3. Results

AmB and cholesterol (mixed at 2:1 ratio) incorporated into artificial phospholipid bilayer membranes that were formed on the tip of patch pipettes and subjected to electrophysiological studies exhibited ion channel current fluctuations with distinct open and closed states (Fig. 2A). Amplitude distribution analysis (Fig. 2B) of the ion channel current trace in Fig. 2A indicates that each state we observed had distinct subpopulations of current levels that were statistically significant. Statistical means derived from Gaussian fits ($r^2 = 0.991$) of the subpopulations show that the ion channels had a net current of 31.4 ± 0.1 pA and a calculated relative conductance of approximately 190 pS. A careful analysis of similar current traces revealed the distinct states (closed, open level 1, and open level 2) and current fluctuation levels corresponding
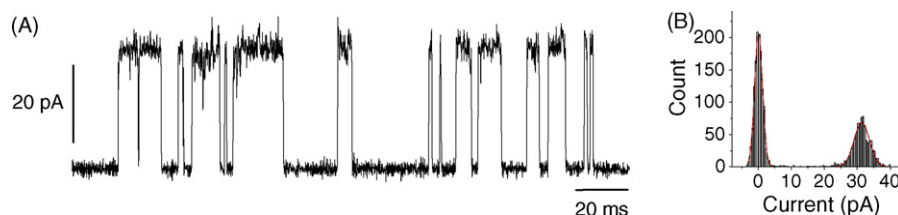

Fig. 2. AmB–cholesterol channels in reconstituted lipid bilayer membranes. Ion channel current fluctuation were elicited by AmB–cholesterol complexes incorporated into artificial lipid bilayer membranes that were formed on the tip of patch pipettes. The voltage was clamped at +165 mV. Openings are upward. The data traces were sampled at 0.1 ms intervals, filtered at 5 kHz, and plotted as a function of time. Panel A shows a 210 ms data trace consisting of 2100 data points. Amplitude distribution of channel currents in panel A is shown in panel B. The trace containing 2100 data points was segmented with a bin width of 0.5 pA and plotted as a function of channel current. The distribution was fitted with the sum of two Gaussian functions ($r^2 = 0.991$) with population means of 0.06 ± 0.02 (S.E.) pA (channel-closed current level) and 31.34 ± 0.08 pA (channel-open current level).
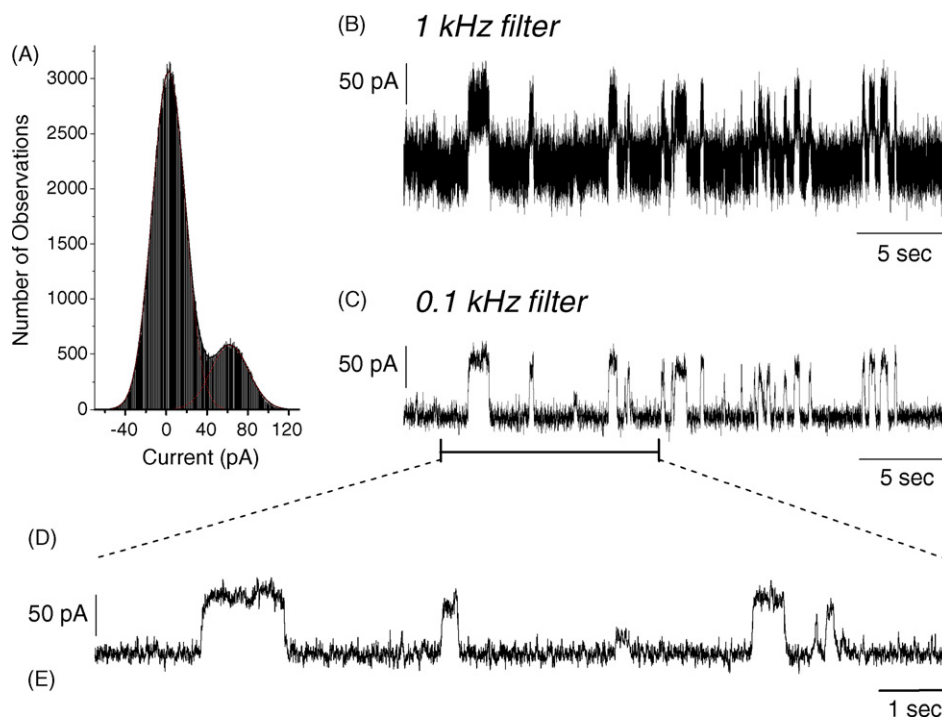
Fig. 3. AmB–cholesterol channels in phospholipid membrane-coated nanoporous silicon surfaces. Ion channel current fluctuations were elicited by AmB–cholesterol complexes that were incorporated in the phospholipid membrane coat of buffer-filled nanoporous (6.5 nm pore diameter) silicon surfaces. The voltage was clamped at +200 mV. Openings are upward. The data traces were sampled at 0.1 ms intervals and plotted as a function of time. Panel B shows a 1 kHz filtered trace of AmB–cholesterol channel currents in phospholipid membrane-coated nanoporous silicon surfaces. The segment is 30 s long and contains 300,000 data points. The corresponding amplitude distribution histogram (panels A) was generated by segmenting the data trace in panel B with a bin width of 0.5 pA and plotting the results as a function of channel current. The histogram was fitted with the sum of two Gaussian functions ($r^2 = 0.999$) with resulting population means of 2.46 ± 0.03 (S.E.) pA and 62.14 ± 0.19 pA, respectively. Panel C shows the same AmB–cholesterol channel current trace in panel B after it has been filtered at 0.1 kHz. Panel D shows an expanded 12 s segment of the 0.1 kHz filtered data trace in panel C and contains 120,000 data points.

to large-conductance and smaller-conductance ion channels (Sykora et al., 2003; Yilma et al., in press).

Based on these findings, we tested the functionality of AmB–cholesterol channels in phospholipid membranes deposited on nanoporous surfaces. Electrophysiological studies of 2:1 AmB–cholesterol mixtures that were incorporated into phospholipid membranes formed on the surface of nanoporous (6.5 nm pore diameter) silicon plates revealed large amplitude ion channel current fluctuations (Fig. 3B–D) with distinct open and closed states. Fig. 3B shows a data trace containing current fluctuations of AmB–cholesterol channels in phospholipid membrane-coated nanoporous silicon surfaces voltage clamped at +200 mV and filtered at 1 kHz. Remarkably, the channels exhibited large relative conductance and high noise level for the baseline. Fig. 3C shows the same trace after the noise was partially filtered out using conventional lowpass Bessel filter set to 0.1 kHz. Amplitude distribution analysis (Fig. 3A) of the ion channel current trace in Fig. 3B indicates that each state we observed had distinct subpopulations of current levels that were statistically significant. Statistical means derived from Gaussian fits ($r^2 = 0.999$) of the subpopulations show that these large-conductance ion channels had a net current of 59.7 ± 0.2 pA and a calculated relative conductance of approximately 300 pS. Fig. 3D depicts an expanded segment of the ion channel current data trace in panel C to better reveal the distinct states (closed level and open level) that were observed in the original data trace.

While performing our experiments, we observed that illuminating the nanoporous silicon surfaces with a light source generated a photovoltaic potential that was measurable in the millivolt range. We further explored this property of the nanoporous silicon surfaces by illuminating similarly prepared phospholipid membrane-coated nanoporous silicon surfaces with a narrow laser beam from a 635 nm diode laser. The approximate voltage generated by the nanoporous silicon surfaces in our experiments varied between samples, and ranged from −80 to −190 mV (data not shown). This was noticeably greater than voltage generated by nonporous (smooth) silicon surfaces.

We utilized the photovoltaic potential generated by nanoporous silicon surfaces to test if the voltage can be utilized to drive ions through a channel incorporated in the lipid membrane coating the nanoporous silicon surfaces. Fig. 4 shows currents observed from AmB–cholesterol containing membrane-coated nanoporous silicon surfaces upon illumination by a narrow laser beam. The responses exhibited initial negative current spikes at the point of laser activation that gradually decayed to a semi-steady state for the duration of the laser illumination. Upon close inspection of the current trace, one can appreciate the small ion channel fluctuations in the steady state current during the period of laser illumination. Panels B and D show expanded and magnified short segments of the AmB–cholesterol channel current fluctuations observed in the steady state current during the period of laser illumination. The channel traces exhibit characteristic
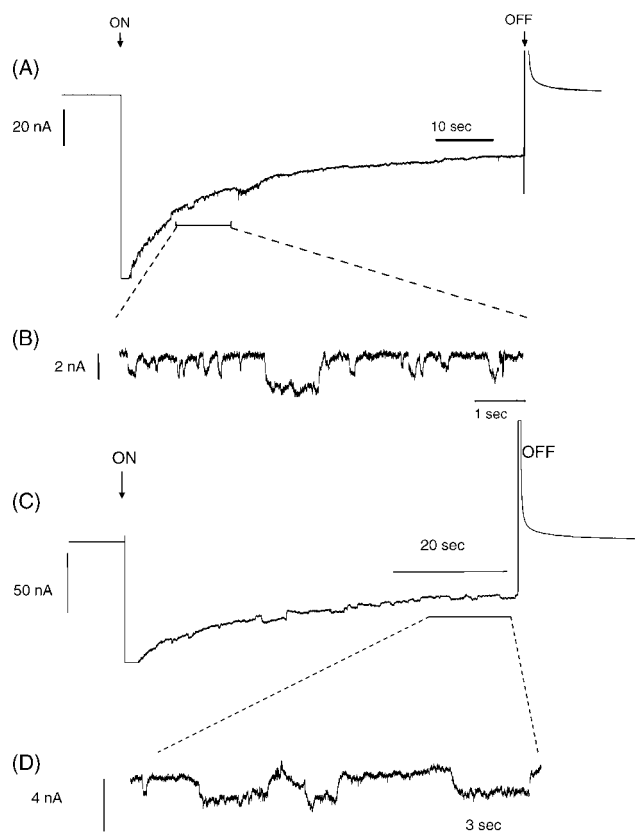
Fig. 4. AmB–cholesterol channels can be driven by voltage generated when the membrane-coated nanoporous silicon surfaces are illuminated by a laser beam. The electrical potential generated when nanoporous silicon surfaces are illuminated by a narrow laser beam was used to drive ions through AmB–cholesterol channels that were incorporated in phospholipid membrane coat of the nanoporous silicon surfaces. Points of laser activation and deactivation in the figure are indicated by ON and OFF, respectively. Panels A and C show results of two different experiments containing the current responses that resulted due to voltage generated when the nanoporous silicon surface was illuminated with the laser beam. In both cases the nanoporous silicon surface was illuminated with a beam from 635 nm diode laser for a short period of time (ON to OFF). The resulting AmB–cholesterol channel current fluctuations can be seen in the slowly decaying current transients resulting during the period of laser illumination. Panels B and D show expanded small segments of the AmB–cholesterol channel current fluctuations observed during laser illumination. The expanded segment B was corrected by subtracting the slope of the decaying current transient from the baseline of the response. The segment D was recorded in the plateau region of the decaying current transient.

open and closed current fluctuations that are indicative of functional ion channels.

4. Discussion

Recent efforts to construct ion-channel-based stochastic sensors (Bayley et al., 2000; Schuster et al., 1998; Gu et al., 1999) have described on the potential ion channels hold for use as transducers in biosensors. However, this effort has just began addressing the need to devise a stable medium for supporting these ion channels while enabling the rapid lateral movement of ions through the medium, as well as constructing a micro-array (Bayley and Cremer, 2001) that is practical and inexpensive. So far, a considerable amount of the ion channels observed on silicon substrates have been in lipid bilayer membranes formed on microfabricated apertures (Pantoja et al., 2001; Peterman et al., 2002; Urisu et al., 2005; Wilk et al., 2004).

Our previous works (Sykora et al., 2003; Yilma et al., in press) have shown that AmB–cholesterol channels can function in phospholipid bilayer membranes formed on the tips of patch pipettes as well as in phospholipid membrane-coated nanoporous silicon surfaces. Our observations of the functioning of these channels in membrane-coated nanoporous silicon surfaces (Lu et al., 1997; Brinker et al., 1999) indicate that such substrates provide a practical medium for supporting ion channels and ion-channel-based stochastic sensors (Bayley and Cremer, 2001). The small nano-pores can provide a reservoir for the ionic/buffer solution and help to stabilize the ion channels. Similar to the results we obtained in tip–dip membranes, voltage-clamp studies of AmB–cholesterol channels in phospholipid membrane-coated nanoporous silicon surfaces revealed large channels with $\sim$300 pS relative conductance. The baseline noise observed from these phospholipid membrane-coated nanoporous silicon surfaces was considerably higher than the baseline noise in tip–dip membranes. Understandably, this phenomenon was due to the increased total phospholipid membrane surface area, capacitance of pores, and the seal resistance (Rudy and Iverson, 1992) in the nanoporous surfaces compared to the significantly smaller surface area of singular tip–dip membranes. Still, with additional filtering, the baseline membrane noise can be reduced to better reveal the channel current fluctuations.

Large conductance AmB–cholesterol channels were dominant in the phospholipid membrane-coated nanoporous silicon surfaces. This could be attributed to two factors. The small surface area of the membranes in the individual nanopore structures could serve to promote/support larger conductance channels by physically crowding smaller channels in favor of larger channels (up to a certain size) which have a smaller circumference to pore-size ratio. Conversely, the current fluctuations of smaller channels that were present in the medium could have been concealed by the high baseline membrane noise, and subsequently eliminated as artifacts during additional filtering. This emphasizes the importance of employing high conductance ion channels to overcome a low signal to noise ratio in ion-channel-based biosensor.

Tackling the issue of addressability generally meant constructing surfaces/substrates that contain elaborate microcircuitry that electrically connect each individual grid to a signal amplifier via separate wires (Bayley and Cremer, 2001). Unfortunately, this approach was both labor-intensive as well as expensive to manufacture. Our approach remedied this problem by utilizing the photovoltaic property of the nanoporous silicon surfaces to generate a localized potential that can drive ions through AmB–cholesterol channels (or any other channels of interest). In the past, this property of silicon substrates was treated as a nuisance by various groups since it was a source of noise and created a necessity to conduct the experiments in the dark (Peterman et al., 2002). Illuminating the phospholipid membrane-coated nanoporous silicon surface with a narrow laser beam generates a localized potential that functions to drive ions through the channels incorporated in the phospholipid

membrane coat. The resulting current can be measured using a single reference/ground electrode and a single recording electrode without losing addressability. Assuming that engineered ion channels with predetermined target-ligand specificities have been applied to a membrane-coated nanoporous silicon surface in a predefined grid pattern, then one can use a narrow laser beam to interrogate specific grids in order to determine if the target ligand has bound. Binding would generally be detected by observing ion channel currents that would result from the movement of ions through the channel that has bound its target ligand. Utilizing computational neural networks, the location of the activated ion channel in the array can be translated to identify the detected compound (Bayley and Cremer, 2001). The results we obtained by driving ions through AmB–cholesterol channels using a photovoltaic potential show that this technique is a practical means of making ion-channel-based biosensors on silicon substrates addressable. Membrane-coated nanoporous silicon surfaces show great promise for use as mediums for ion-channel-based biosensors as well as for organization in sensor arrays.

A photovotaic driving force across a biological or synthetic membrane can be utilized in a variety of areas. For example, application of a localized voltage across a membrane can be used to address or map biological structures such as ion channels and/or to detect binding events at a channel. AmB ion channel within a supporting membrane, for example, is held open by a cholesterol molecule that zips the amphotericin molecules together in a channel-forming configuration, allowing ion transport through the membrane (Fig. 5A). When a free analyte binds to cholesterol-linked antibodies, the cholesterol molecule

is displaced and the channel is unzipped, resulting in disaggregating and closing of the channel, thereby blocking ion transport across the membrane (Fig. 5B) (Cornell et al., 1997). Similarly, a nanopore-wafer-based biosensor can be coated with a diverse selection of ligand-gated ion channels (acetylcholine receptor, glutamate receptor, etc.). The ion channel will remain closed when no ligand/analyte is bound (Fig. 5C). However, when the surface of this chip is exposed to minute amounts of the specific ligand, one group of these channels (that respond specifically to the ligand) will open allowing for the movement of millions of ions per second, thereby amplifying individual binding events to electrically detectable levels (Fig. 5D). The technique enables precise location control of the point of application of voltage across a membrane, providing improved addressing of ion channels and improved detection of binding events at a channel. It can also provide photoelectric power supply, microswitching, energy transmission and/or signal transmission suitable for use in connection with nanodevices including nanomotors, nanoswitches, and nanopositioners.
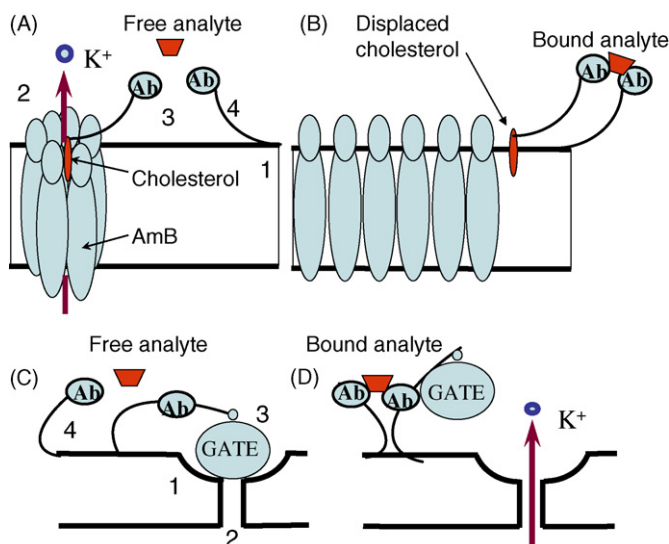
Fig. 5. Schematic diagrams of AmB ion channel biosensor. (A and B) Normally open channel biosensor. (A) Open AmB channel. (1) Supporting membrane, (2) AmB channel, (3) recognition molecule (antibody or peptide) linked to a cholesterol gate and (4) molecular anchor (the same recognition molecule linked to membrane surface). (B) Closed disaggregated channel. (C and D) Normally closed channel biosensor. (C) Channel closed by gate. (1) Supporting membrane, (2) ion channel, (3) gate with recognition molecule attached to the supporting membrane. (4) Molecular anchor (the same recognition molecule linked to membrane surface).

References

Anrather, D., Smetazko, M., Saba, M., Alguel, Y., Schalkhammer, T., 2004. J. Nanosci. Nanotechnol. 4 (1/2), 1–22.

Bayley, H., Braha, O., Gu, L.Q., 2000. Adv. Mater. 12, 139–142.

Bayley, H., Cremer, P.S., 2001. Stochastic sensors inspired by biology. Nature 413, 226–230.

Becucci, L., Guidelli, R., Peggion, C., Toniolo, C., Moncelli, M.R., 2005. J. Electroanal. Chem. 576 (1), 121–128.

Bolard, J., 1986. Biochim. Biophys. Acta 864, 257–304.

Borisova, M.P., Ermishkin, L.N., Silberstein, A.Y., 1979. Biochim. Biophys. Acta 553, 450–459.

Brinker, C.J., Lu, Y., Sellinger, A., Fan, H., 1999. Adv. Mater. 11, 579–585.

Brutyan, R.A., McPhie, P.J., 1996. J. Gen. Physiol. 107, 69–78.

Cornell, B.A., Braach-Maksvytis, V.L., King, L.G., Osman, P.D., Raguse, B., Wieczorek, L., Pace, R.J., 1997. Nature 387 (6633), 580–583.

Ermishkin, L.N., Kasumov, K.M., Potseluyev, V.M., 1977. Biochim. Biophys. Acta 470, 357–367.

Ermishkin, L.N., Kasumov, Kh.M., Potseluyev, V.M., 1976. Nature 262, 698–699.

Gong, J.-M., Lin, X.-Q., 2003. Chin. J. Chem. 21 (7), 756–760.

Gu, L.Q., Braha, O., Conlan, S., Cheley, S., Bayley, H., 1999. Nature 398, 686–690.

Hartsel, S.C., Bolard, J., 1996. Trends Pharmacol. Sci. 17, 445–449.

Holz, R., Finkelstein, A., 1970. J. Gen. Physiol. 56, 125–145.

Kerridge, D., Whelan, W.L., 1983. In: Trinici, A.P.J., Ryley, J.F. (Eds.), Mode of Action of Anti-fungal Agents. Cambridge University Press, Cambridge, pp. 343–375.

Lu, Y., Ganguli, R., Drewien, C.A., Anderson, M.T., Brinker, C.J., Gong, W.L., Guo, Y.X., Soyez, H., Dunn, B., Huang, M.H., Zink, J.I., 1997. Nature 389, 364–368.

Ma, C., Srinivasan, M.P., Waring, A.J., Lehrer, R.I., Longo, M.L., Stroeve, P., 2003. Coll. Surf. B: Biointerf. 28 (4), 319–329.

Pantoja, R., Sigg, D., Blunck, R., Bezanilla, F., Heath, J.R., 2001. Biophys. J. 81, 2389–2394.

Peterman, M.C., Ziebarth, J.M., Braha, O., Bayley, H., Fishman, H.A., Bloom, D.M., 2002. Biomed. Microdev. 4, 231–236.

Rudy, B., Iverson, L.E., 1992. Ion Channels, Methods in Enzymology, vol. 207. Academic Press, pp. 45–48.

Schuster, B., Pum, D., Braha, O., Bayley, H., Sleytr, U.B., 1998. Biochim. Biophys. Acta 1370, 280–288.

Suppiramaniam, V., Bahr, B.A., Sinnarajah, S., Owens, K., Rogers, G., Yilma, S., Vodyanoy, V., 2001. Synapse 40, 154–158.

Sykora, J., Yilma, S., Neely, W.C., Vodyanoy, V., 2003. Langmuir 19, 858–864.

Urisu, T., Rahman, M., Uno, H., Tero, R., Nonogaki, Y., 2005. Nanomedicine 1 (4), 317–322.

Vodyanoy, V., 1998. Olfactory sensor. In: Proceedings of the 10th Annual International Conference on IEEE Engineering in Medicine and Biology Society, vol. 10, pp. 997–998.

Vodyanoy, V., Bahr, B.A., Suppiramaniam, V., Hall, R.A., Baudry, M., Lynch, G., 1993. Neurosci. Lett. 150, 80–84.

Wilk, S.J., Goryll, M., Laws, G.M., Goodnick, S.M., Thornton, T.J., Saraniti, M., Tang, J., Eisenberg, R.S., 2004. Appl. Phys. Lett. 85 (15), 3307–3309.

Yilma, Sykora, J.C., Samoylov, A., Lo, T., Liu, N., Brinker, C.J., Neely, W.C., Vodyanoy, V., in press. Biosens. Bioelectron.